

1 **A critical assessment of widely used techniques for nitrate source**  
2 **apportionment in arid and semi-arid regions.**

3 **V. Re<sup>a, b\*1</sup>, S. Kammoun<sup>b</sup>, E. Sacchi<sup>c</sup>, R. Trabelsi<sup>b</sup>, K. Zouari<sup>b</sup>, I. Matiatos<sup>d</sup>, E. Allais<sup>e</sup>, S. Daniele<sup>a</sup>**

4 <sup>a</sup> Department of Molecular Sciences and Nanosystems, Ca' Foscari University of Venice, Via Torino  
5 155, 30170 Venezia-Mestre, 40123 Venice, Italy

6 <sup>b</sup> Laboratory of Radio-Analyses and Environment, National School of Engineers of Sfax, BP1173,  
7 3038 Sfax, Tunisia

8 <sup>c</sup> Department of Earth and Environmental Sciences, University of Pavia, Via Ferrata 9, 27100 Pavia,  
9 Italy

10 <sup>d</sup> Isotope Hydrology Section, International Atomic Energy Agency, Vienna International Centre, PO  
11 Box 100, A-1400, Vienna, Austria

12 <sup>e</sup> ISO4 s.n.c., via Valperga Calus 35, 10125, Turin, Italy

13 \*Corresponding author email: [viviana.re@unipi.it](mailto:viviana.re@unipi.it)

14

15 **Abstract-** The assessment of nitrate pollution origin using stable isotope techniques is a  
16 fundamental prerequisite for the application of sustainable groundwater management plans.  
17 Although nitrate pollution is a worldwide groundwater quality problem, existing knowledge on the  
18 origin of nitrate pollution in arid and semi-arid regions is still scarce. Using the example of the  
19 Grombalia aquifer (NE Tunisia), this work summarizes the main strengths and constraints of multi-  
20 isotope techniques targeting at nitrate source identification and apportionment. The results  
21 highlighted that, even in the case of well-established methodologies, like those of isotope  
22 hydrogeochemistry ( $\delta^{15}\text{N}_{\text{NO}_3}$ ,  $\delta^{18}\text{O}_{\text{NO}_3}$  and  $\delta^{11}\text{B}$ ) and mixing modelling for source apportionment, it  
23 is fundamental to take into account regional and local end-members to avoid biased data  
24 interpretation and to fully exploit the potential of such accurate tools.

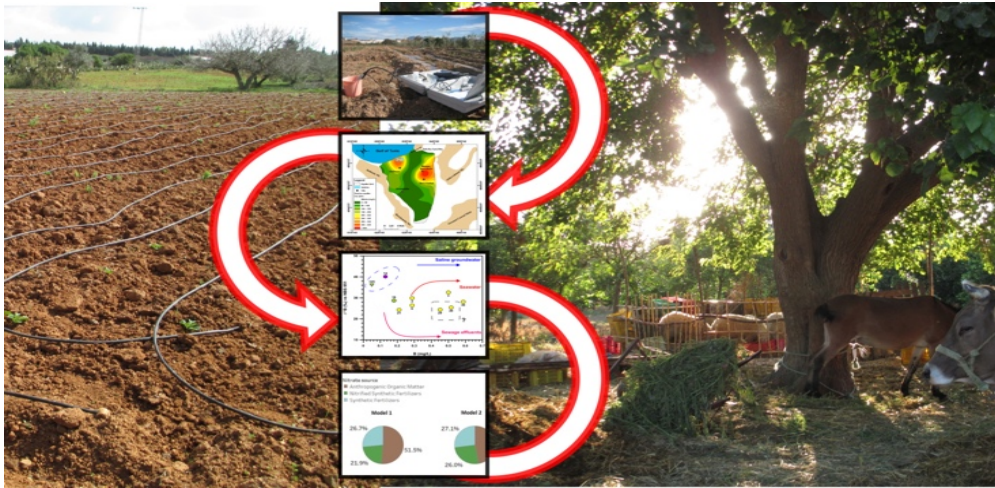
---

<sup>1</sup> PRESENT ADDRESS: *Department of Earth Sciences, University of Pisa, Via S. Maria 53, 56126, Pisa, Italy*

25 **Keywords:** Groundwater, hydrogeochemistry, isotopes, mixing models

26

27 **Graphical Abstract.**



28

29

30

31

32

33

## 34 **Introduction**

35 Nitrate contamination of groundwater bodies is a widely acknowledged environmental and public  
36 health issue, although the correct procedure to be adopted for source identification is still an open  
37 question, especially when multiple sources (urban and rural) are present (Spalding and Exner, 1993).  
38 In arid and semiarid regions (A&SAR), groundwater is often characterized by high salinity (Greene  
39 et al., 2016; Jalali, 2007; Leduc et al., 2018) and diffuse nitrate contamination (Alsharhan and Rizk,  
40 2020; Gutiérrez et al., 2018), with mutually interacting processes. Indeed, even if the anthropogenic  
41 recharge by sewage and irrigation water has a negligible effect in terms of salinity input, the  
42 associated nitrate content fuels up water-rock interaction processes, eventually leading to a further  
43 mineralization increase. This mechanism makes nitrate source apportionment even more difficult  
44 with hydrochemical and isotopic tools (Re and Sacchi, 2017). In addition, it is of paramount  
45 importance not only to correctly identify the pollution source(s), but also to assess the  
46 predominance of one source over another, if a simultaneous contribution of multiple sources occur.  
47 This can be estimated using isotope mass-balance mixing models, which are based on  $\delta^{15}\text{N-NO}_3$  and  
48  $\delta^{18}\text{O-NO}_3$  values (Deutsch et al., 2006; Phillips and Gregg, 2003; Phillips and Koch, 2002; Voss et al.,  
49 2006). The application of these models has proved to be complicated especially in the case of diffuse  
50 contamination, because of the temporal and spatial variability in  $\delta^{15}\text{N}$  and  $\delta^{18}\text{O}$  of  $\text{NO}_3$ , and the  
51 possible isotope fractionation processes (e.g. denitrification) that alter the isotopic composition of  
52 the initial source signal and the chemical concentrations of Nitrogen species (Moore and Semmens,  
53 2008; Xue et al., 2009a). Additional parameters like  $\delta^{11}\text{B}$  may help overcome the difficulty of  
54 overlapping nitrate isotope signatures. The rationale for a coupled use of B and N isotopes is that  
55 these elements have the same anthropogenic origin and co-migrate in the groundwater.  
56 Nevertheless, boron is always present at a background concentration that mostly depends on the  
57 aquifer matrix, influencing also its isotopic composition and potentially masking the signature of the

58 anthropogenic input (Martinelli et al., 2018; Re and Sacchi, 2017) . Bayesian-based stable isotope  
59 mixing models, like SIAR or MixSIAR (Parnell et al., 2010; Stock et al., 2018), have been widely used  
60 to determine the probability distribution of the proportional contribution of each nitrogen source  
61 to a mixture and to overcome the constraints mentioned above (e.g. (Matiatos, 2016; Meghdadi  
62 and Javar, 2018; Xia et al., 2017; Yang et al., 2013; Zhang et al., 2018)). Results of these models are  
63 strongly dependent on the values assumed for  $\delta^{15}\text{N}_{\text{NO}_3}$  and  $\delta^{18}\text{O}_{\text{NO}_3}$  of the contamination sources.  
64 Comparing field data with the compositional ranges reported in the literature (e.g. (Kendall et al.,  
65 2008; Kendall and Aravena, 2000)) can provide useful insights on the possible sources of  
66 contaminations. However, given the recent increase in studies addressing  $\text{NO}_3$  contamination and  
67 the growing accessibility of analytical techniques, the compositional ranges classically reported in  
68 the  $\delta^{18}\text{O}_{\text{NO}_3}$  -  $\delta^{15}\text{N}_{\text{NO}_3}$  biplot are getting broader and often overlapping. This can make difficult the  
69 interpretation unless one carries out a more in-depth analysis by comparing the results of similar  
70 geographic and climatic areas. Finally, little is known about the real effectiveness of this approach  
71 in A&SAR, due to the potential modifications of the isotopic input signal related to the long N  
72 residence time in soils (Craine et al., 2015).

73 A&SAR cover almost the 41% of Earth's land surface and are home for approximately 35% of the  
74 global population (Mortimore et al., 2009). In these areas, groundwater often represents the main  
75 freshwater source to support local populations' development (Re and Zuppi, 2011), and climate  
76 changes may further reduce its availability, as per the increase of the length of dry season and  
77 extreme droughts events (IPCC, 2021). Hence, the identification of the proportional contribution of  
78 nitrate sources is essential to control nitrate pollution and to develop effective management  
79 practices.

80 This paper aims at evaluating the effectiveness of the more widely used approaches targeted to the  
81 identification of nitrate contamination origin in A&SAR, when multiple inputs are present and the

82 long-term sustainability of groundwater resources is at stake. To this end, a case study,  
83 representative of typical nitrate contamination issues Mediterranean coastal aquifer is presented:  
84 the Grombalia aquifer (Tunisia).

85

## 86 **Material and methods**

### 87 **Study area**

88 The Grombalia coastal aquifer (Tunisia) covers a surface of 719 Km<sup>2</sup>. It is constituted by a shallow  
89 aquifer, with an average thickness of about 50 m, hosted in the Quaternary continental sand, clayey  
90 sand and sandstones deposits, and multilayers confined aquifer with average thickness of about 100  
91 m communicating through discontinuities (Castany, 1948). The recharge in the shallow unconfined  
92 aquifer mainly occurs in the pediments of the surrounding mountains and converges to the central  
93 part of the basin. There, a general southeast–northwest flow carries groundwater to the Gulf of  
94 Tunis discharge areas (Ben Moussa et al., 2010; Gaaloul et al., 2014).

95 The Grombalia aquifer is located in one of the most important agricultural regions in the country,  
96 and groundwater is often used for both irrigation and domestic consumption (Tringali et al., 2017).

97 However, the high salinity and nitrate concentrations make the shallow aquifer unsuitable for  
98 human use without treatment (Ben Moussa and Zouari, 2011; Charfi et al., 2013; Kammoun et al.,  
99 2018b), as many other aquifers in the country and in the Mediterranean basin (Leduc et al., 2018).

100 Recently, (Re et al., 2017) demonstrated that high nitrate concentrations are present also in the  
101 deeper aquifer, generally considered less vulnerable to pollution, and that synthetic fertilizers are  
102 not the only source of nitrate contamination, pointing out the dual impact of both agricultural and  
103 domestic sources. However, so far no study permitted to distinguish between manure and sewage  
104 input, nor to determine the proportional contribution of each nitrate source to groundwater of

105 these systems. The latter would be a crucial point to devise adequate new policies and management  
106 strategies for preventing the aquifer from further contamination.

107

### 108 **Hydrochemical and isotopic analyses**

109 A total of 116 samples were collected in both the shallow (n=61) and deep (n=55) Grombalia  
110 aquifers in different campaigns (February 2014, September 2014 and March 2015; Figure S1), to  
111 assess the possible occurrence of seasonal variations and changes in groundwater quality. *In situ*  
112 measurements of electrical conductivity, pH and water temperature were performed, using a WTW  
113 340i multimeter. Samples for major ion analysis were filtered through 0.45 µm cellulose membrane  
114 and stored in high density polyethylene bottles. Chemical and isotopic analyses of the water  
115 samples were performed at the Laboratory of Radio-Analyses and Environment (LRAE) of the  
116 National School of Engineers of Sfax (Tunisia). Major elements were analysed using a Dionex DX 100  
117 ion chromatograph equipped with a CS12 and an AS14A-SC Ion Pac columns and an AS-40auto-  
118 sampler. The total alkalinity (as  $\text{HCO}_3^-$ ) was determined by titration with standard hydrochloric acid  
119 (0.1 N) using phenolphthalein and methyl orange and as indicators. The error, based on the charge  
120 balance, was calculated to be < 5%. Analyses of the stable isotopes of the water molecule ( $\delta^2\text{H}$  and  
121  $\delta^{18}\text{O}$ ) were performed using the Laser Absorption Spectrometer LGR DLT 100 (Penna et al., 2010).  
122 Results are reported in ‰ vs. SMOW (Standard Mean Oceanic Water) with an analytical error  $\pm 1$   
123 for  $\delta^2\text{H}$  and  $\pm 0.1$  for  $\delta^{18}\text{O}$ . The isotopes of dissolved nitrate ( $\delta^{15}\text{N}_{\text{NO}_3}$  and  $\delta^{18}\text{O}_{\text{NO}_3}$ ) were prepared and  
124 analysed at the ISO4 private laboratory (Turin, Italy) using a Finningan™ MAT 250 Mass  
125 Spectrometer, following the procedures described by Silva et al. (Silva et al., 2000). Results are  
126 expressed in ‰ and refer to AIR and V-SMOW (Gonfiantini et al., 1995) with uncertainties ( $2\sigma$ ) of  
127  $\pm 0.5\text{‰}$  and  $\pm 1\text{‰}$  respectively. Boron concentration was determined by ICP-AES. Boron isotopes

128 (expressed as  $\delta^{11}\text{B}\%$  vs NBS951) were determined by MC-ICP-MS at ALS Scandinavia AB, Sweden,  
129 with combined uncertainty ( $1\sigma$ ) of  $\pm 0.4$  to  $\pm 1\%$ .

130

### 131 **Multivariate Statistical Analysis**

132 Statistical data treatment, in the form of Principal Component Analysis (PCA; e.g. (Chatfield, 2018))  
133 and Hierarchical Cluster Analysis (HCA), was performed using the statistical package SPSS 15.0 for  
134 Windows® (SPSS, Inc., Chicago, IL, USA, 2004). PCA was conducted on a total of 115 samples  
135 considering only the hydrochemical and isotopic variables ( $n = 13$ ) common to all samples (pH,  $\text{HCO}_3$ ,  
136 EC, TDS, Cl,  $\text{NO}_3$ ,  $\text{SO}_4$ , Na, K, Mg, Ca,  $\delta^{18}\text{O}$ ,  $\delta^2\text{H}$ ). To increase the efficiency of the PCA, pH and  $\text{HCO}_3$   
137 were excluded from the analysis due to a poor correlation with most of the variables. To reduce the  
138 overlap of the original variables over each principal component a Varimax rotation was  
139 performed (Kaiser, 1958).

140 HCA was conducted using Ward's single linkage method in combination to Euclidean distance, in  
141 order to identify groundwater groups showing similar hydrogeochemical composition.

142

### 143 **Bayesian isotope mixing model**

144 To estimate the proportional contributions of multiple  $\text{NO}_3$  sources, a Bayesian isotope mixing  
145 model was applied using the software package SIAR (Stable Isotope Analysis in R), a language and  
146 environment for statistical computing (Jackson et al., 2009; Moore and Semmens, 2008; Parnell et  
147 al., 2010). For a set of  $N$  mixture measurements on  $J$  isotopes with  $K$  source contributors, the mixing  
148 model is expressed as follows (Equation 1; (Parnell et al., 2010)):

149

150 *Equation 1*

151

152

$$X_{ij} = \sum_{k=1}^K p_k (S_{jk} + C_{jk}) + \varepsilon_{ij}$$
$$S_{jk} \sim N(\mu_{jk}, \omega_{jk}^2)$$

153  $C_{jk} \sim N(\lambda_{jk}, \tau_{jk}^2)$

154  $\varepsilon_{jk} \sim N(0, \sigma_j^2)$

155

156 where  $X_{ij}$  is the isotope value  $j$  of the mixture  $i$ , in which  $i=1, 2, 3, \dots, N$  and  $j=1, 2, 3, \dots, J$ ;  $S_{jk}$  is the source  
157 value  $k$  on isotope  $j$  ( $k=1, 2, 3, \dots, K$ ) and is normally distributed with mean  $\mu_{jk}$  and standard deviation  
158  $\omega_{jk}$ ;  $p_k$  is the proportion of source  $k$ , which needs to be estimated by the SIAR model;  $c_{jk}$  is the isotope  
159 fractionation factor for isotope  $j$  on source  $k$  and is normally distributed with mean  $\lambda_{jk}$  and standard  
160 deviation  $\tau_{jk}$ ; and  $\varepsilon_{ij}$  is the residual error representing the additional unquantified variation between  
161 individual mixtures and is normally distributed with mean 0 and standard deviation  $\sigma_j$ . More  
162 information about the model can be found in (Jackson et al., 2009; Moore and Semmens, 2008).

163

## 164 **Results and Discussion**

165 This section is organized so as to follow the most commonly adopted investigation approaches, in  
166 increasing degree of complexity and analytical cost involved. For each step, the main findings,  
167 uncertainties and criticalities are evidenced, stressing the difficulties encountered when applied to  
168 A&SAR.

169

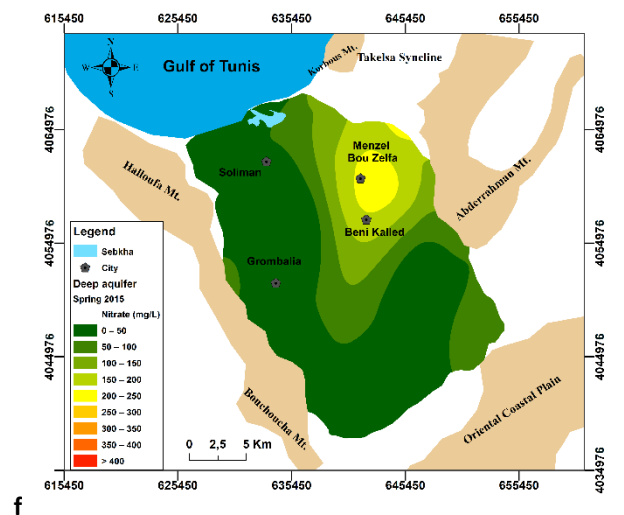
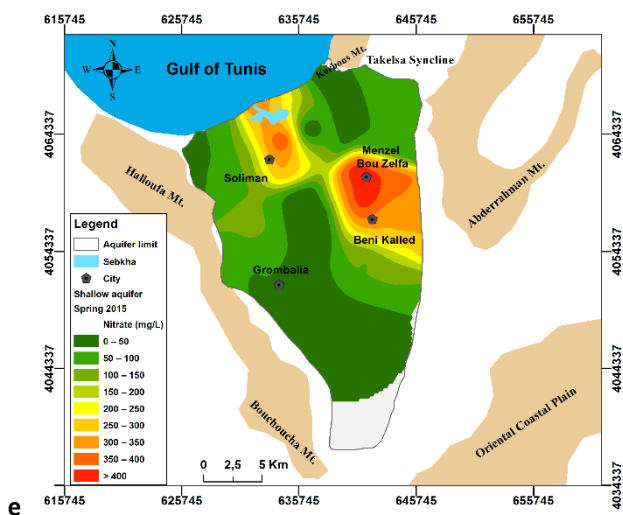
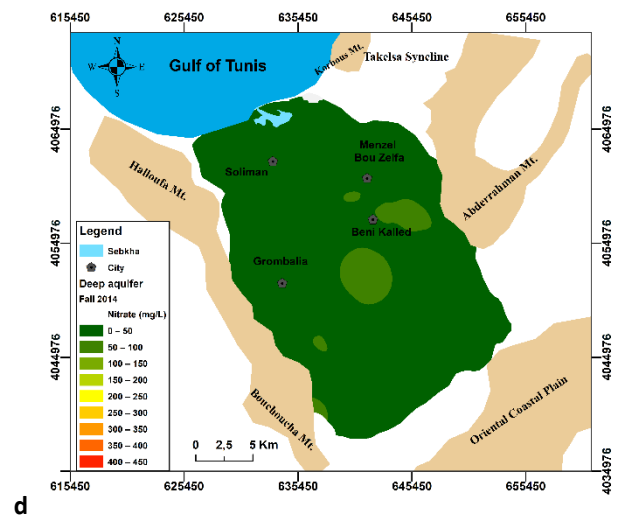
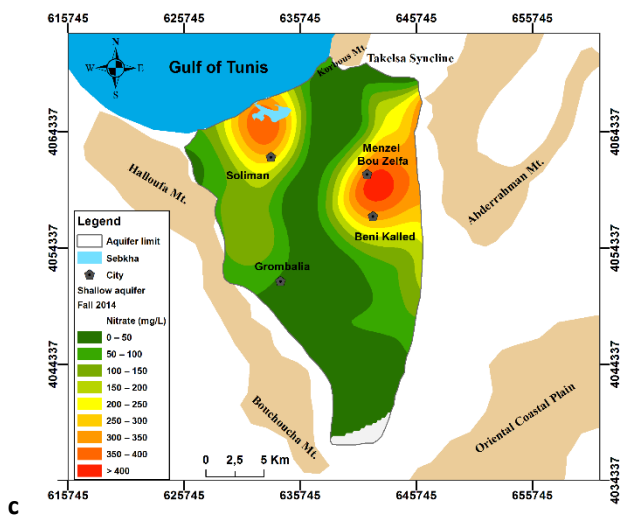
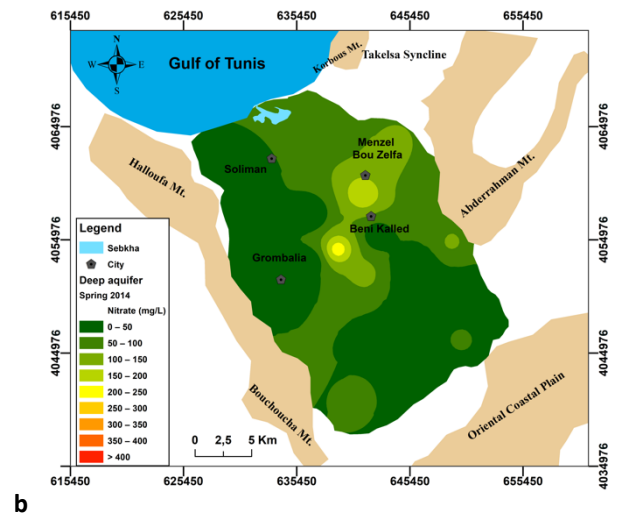
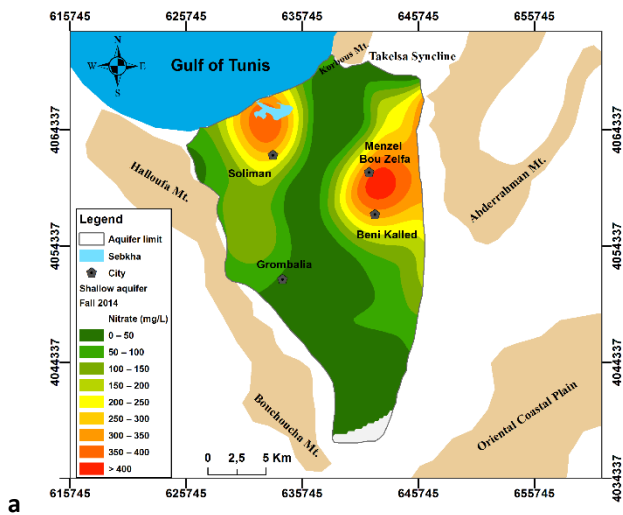
### 170 **The basics: nitrate contents and distribution**

171 The hydrogeochemical assessment confirms that high nitrate concentrations characterize both the  
172 shallow and the deep aquifers regardless to the season and/or irrigation periods (Table S1). Overall,  
173 approximately 51% of the samples (62% in the shallow aquifer and 38% in the deep one) are  
174 unsuitable for drinking water purposes, having concentrations exceeding the statutory limits set by  
175 the WHO (50 mg[NO<sub>3</sub><sup>-</sup>]/L (WHO, 2011)).

176 These findings are in line with the observed nitrate concentration increase, commonly observed in  
177 the past decades in aquifers from A&SAR, due to anthropogenic inputs (Gutiérrez et al., 2018).



178 Results also highlight the presence of two pollution hotspots, common to both the shallow and the  
179 deep aquifers, as suggested by (Re et al., 2017) (Figure 1). The first one is located in the central part  
180 of the plain, in an area identified by (Chenini et al., 2015) as at high to very high groundwater  
181 contamination risk, due to the dominance of irrigated areas. The second hotspot is located along  
182 the coast, where urban settlements and industrial activities prevail. While this seems to suggest the  
183 dominance of only two contamination sources (agriculture and urban/domestic activities), the lack  
184 of sanitation facilities in some rural and peri-urban zones represents another potential  
185 anthropogenic contribution to nitrate pollution in the region (Re et al., 2017). The latter can be  
186 hardly discriminated by solely integrating hydrochemical and land use information. The similarity in  
187 the distribution of pollution hotspots in both aquifers suggests their interconnection and highlights  
188 their vulnerability.



189 Figure 1. Nitrate concentrations (in mg/L) distribution maps in the different sampling seasons: a) shallow aquifer, spring 2014; b)  
 190 deep aquifer, spring 2014; c) shallow aquifer, fall 2014; d) deep aquifer, fall 2014; e) shallow aquifer, spring 2015; f) deep aquifer,  
 191 spring 2015.

192 **Multiparametric approach: advanced statistical analysis**

193 PCA was performed to support geochemical evidences and to identify common patterns among  
194 samples. The value of 2183.76 for the Barlett's chi-square sphericity test (55 degrees of freedom  
195 and a minimum significance level of 0.00) indicates the existence of a statistically significant  
196 interrelationship between variables. Moreover, the measure of sampling adequacy obtained by the  
197 Kaiser Meyer Olkin statistic returns a rather high value (0.710), validating the PCA application. From  
198 the analysis, two varifactors (VF) were extracted (Table S2, Figure 2a), explaining 78.6% of the total  
199 variance, and supporting the hypothesis of the co-existence of two main processes dominating  
200 groundwater hydrogeochemistry: salinization and NO<sub>3</sub> pollution.

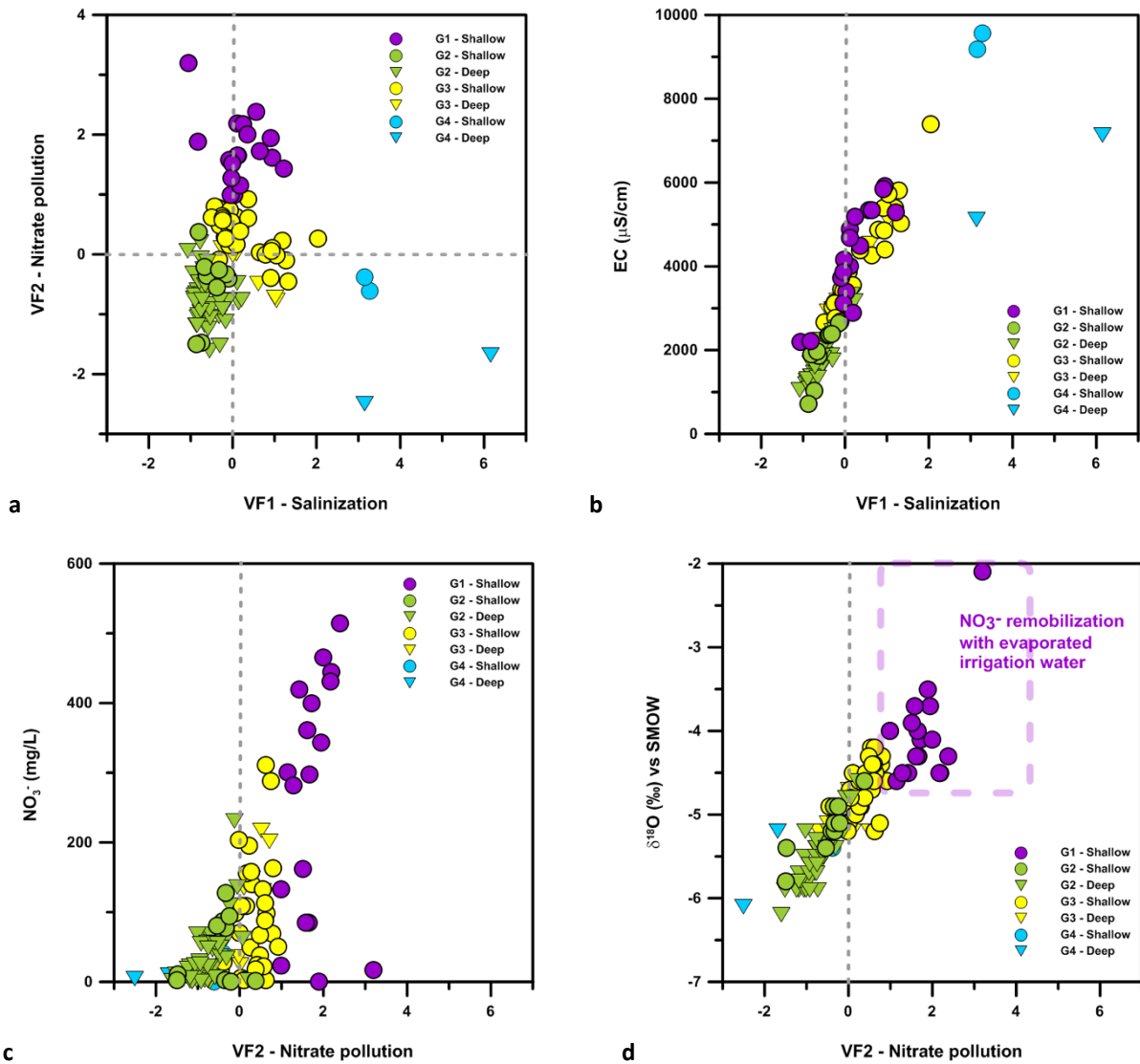
201 In particular, VF1, accounting for 60.4% of the total variance, indicates a strong positive correlation  
202 of EC, TDS, Cl, SO<sub>4</sub>, Na, K, Mg, Ca, and is interpreted as the salinization component, attributable to  
203 water-rock interaction processes and seawater intrusion. This result is in agreement with literature  
204 data (e.g. (Gaaloul et al., 2014; Re et al., 2017; Slama and Sebei, 2020)) highlighting that natural  
205 salinity can be associated to the dissolution of evaporites throughout the plain, and to saline  
206 intrusion in the shallow wells near to the coast.

207 On the other hand, the second component (VF2), explaining 18.2% of the total variance, shows a  
208 strong correlation with  $\delta^2\text{H}$ ,  $\delta^{18}\text{O}$ , and NO<sub>3</sub>. This factor is representative of nitrate pollution, either  
209 associated to direct NO<sub>3</sub> input (e.g. fertilizers, manure and sewages), or to the remobilization of NO<sub>3</sub>  
210 stocked in the unsaturated zone associated to irrigation activities (i.e. return flow of evaporated  
211 irrigation waters, explaining the correlation between isotopic enrichment and NO<sub>3</sub> concentrations  
212 in VF2).

213

214

215



216 Figure 2. Relationship between the varifactors related to HCA groups (Ward method) and the main variable they represent. a) VF2  
 217 ( $\text{NO}_3^-$  pollution) versus VF1 (Salinization); b) Electrical Conductivity (EC) versus VF 1; c)  $\text{NO}_3^-$  concentration versus VF2; d)  $\delta^{18}\text{O}$  versus  
 218 VF2.

219

220 The HCA permitted to classify the samples into four groups (Table S1), and this classification was  
 221 used to further constraint the dominant process in each sample (Figure 2):

- 222 • The first group (G1; 15.5% of the samples) includes the samples where  $\text{NO}_3^-$  remobilization  
 223 associated to irrigation practices dominates, as evidenced by the highest scores for  $\delta^{18}\text{O}_{\text{H}_2\text{O}}$ .  
 224 Interestingly, this cluster includes only shallow well samples (29.5% over the total samples  
 225 collected in the shallow aquifer), highlighting the previously mentioned high vulnerability to  
 226 pollution of the shallow aquifer.

- 227 • On the other hand, most of the samples collected in the deep aquifer (77.8%) fits in a second  
228 group (G2; 45% of the total samples) characterized by more negative  $\delta^{18}\text{O}$  and  $\delta^2\text{H}$  values,  
229 negative values of both VF1 and VF2, and lower average  $\text{NO}_3$  concentrations (38.4 mg/L).  
230 Additionally, the 33.3% of the deep aquifer samples belonging to this group show  $\text{NO}_3$   
231 concentrations exceeding the statutory limit for drinking waters (maximum concentration =  
232 230.6 mg/L). This result confirms the vulnerability of the deeper aquifer, also evidenced by the  
233 general chemistry, and points out that nitrate pollution origin in the deep aquifer should be  
234 attributed to a different process than  $\text{NO}_3$  remobilization.
- 235 • The third group (G3; 35.6% of the samples) does not show a clear dominance of salinization nor  
236 nitrate pollution. In particular, in this group, 50.1% of the shallow well samples is found,  
237 highlighting common issues affecting aquifers located in A&SAR, where the high natural salinity,  
238 due to evaporation, water rock-interaction processes and/or seawater intrusion (Re et al.,  
239 2017) (Kammoun et al., 2018a), makes difficult the correct discrimination of salinization  
240 sources. Hence, this group could represent samples affected by mixing processes, without a  
241 remarkable dominance.
- 242 • As concerns salinization, this process appears to be dominant over  $\text{NO}_3$  pollution only in 4 points  
243 out of 115 (G4).

244 In summary, while the multiparametric statistical approach permits to further highlight the  
245 previously mentioned direct and indirect contribution to nitrate pollution, it is less performant to  
246 correctly discriminate among the dominant processes affecting samples' composition (i.e. natural  
247 versus anthropogenic salinization), and hence may not be sufficient to provide information for the  
248 correct identification of nitrate pollution sources.

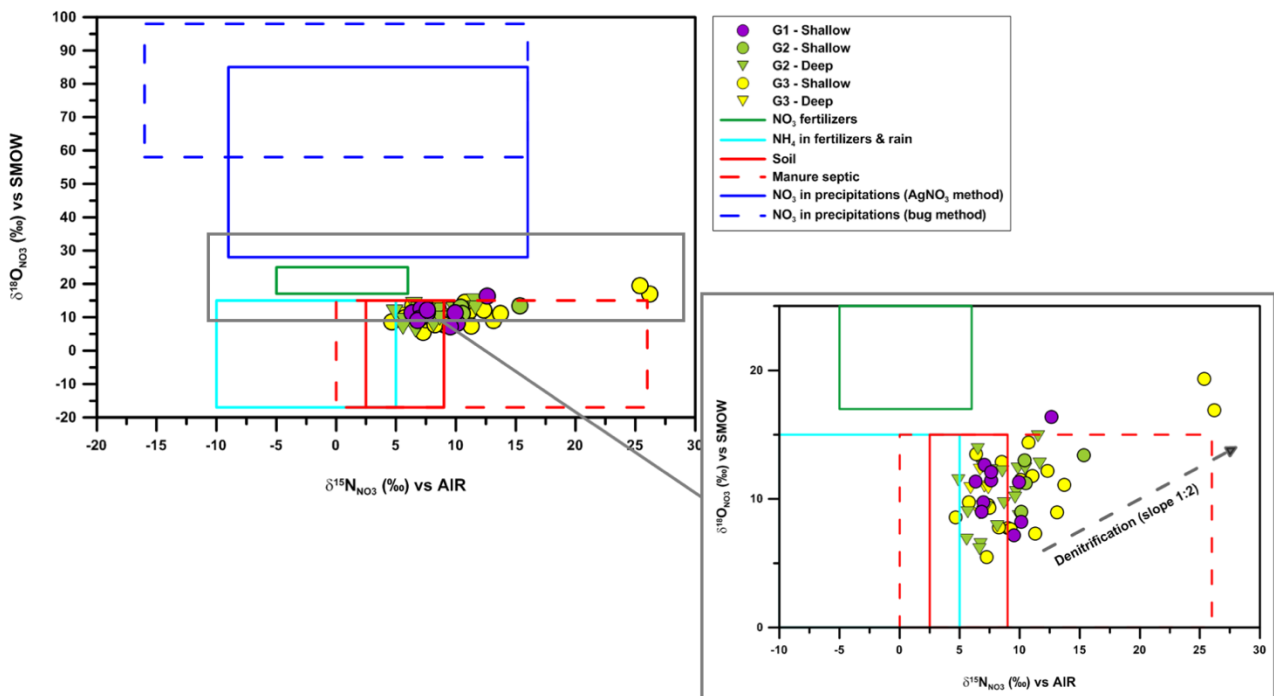
249

250

251 **In-depth analysis: multi-isotopic assessment**

252 In investigations targeted to constraint nitrate pollution origin, the dual nitrate isotopes ( $\delta^{15}\text{N}_{\text{NO}_3}$   
253 and  $\delta^{18}\text{O}_{\text{NO}_3}$ ) approach is generally recognized to be a quite powerful tool ((Re and Sacchi, 2017) and  
254 references therein). By comparing  $\delta^{15}\text{N}_{\text{NO}_3}$  and  $\delta^{18}\text{O}_{\text{NO}_3}$  of the groundwater samples collected in the  
255 Grombalia aquifer with the composition of the main sources reported in the literature (Kendall et  
256 al., 2008) (Figure 3), it is possible to observe that, most of the samples plot in the compositional  
257 range of soil organic matter (regardless of the membership of one of the groups previously identified  
258 with the HCA). However, as pointed out by (Re et al., 2017), due to the  $\text{NO}_3$  concentrations  
259 exceeding the expected natural background level (10-12 mg/L (Edmunds and Shand, 2009; Sacchi  
260 et al., 2013)), these samples likely record a mixed contamination from both synthetic fertilizers and  
261 anthropogenic organic matter (animal or human waste). The latter source is characterized by  
262 enriched  $\delta^{15}\text{N}_{\text{NO}_3}$  values, exceeding +10‰; nevertheless, this organic matter contribution may be  
263 considered dominant for samples showing a  $\delta^{15}\text{N}_{\text{NO}_3}$  greater than +8.6‰ (Re and Sacchi, 2017).  
264 These findings, common to many other aquifers in A&SAR (Alsharhan and Rizk, 2020; Danni et al.,  
265 2019; Diédhiou et al., 2012; Favreau et al., 2009; Gutiérrez et al., 2018), highlight the need for a  
266 more specific assessment of  $\text{NO}_3$  isotopic ranges. In particular, the use of locally relevant  $\delta^{15}\text{N}$  source  
267 values is generally recommended (Isonitrate, 2010), but probably still not sufficient to unveil the  
268 specific impact of environmental and climatic conditions to soil organic matter, fertilizers, manure  
269 and sewage during their residence time in the unsaturated zone, prior to groundwater recharge.  
270 (Kendall, 1998) introduced the expected ranges of  $\delta^{15}\text{N}$  and  $\delta^{18}\text{O}$  values of nitrate sources through  
271 visual  $\delta^{18}\text{O}$  vs  $\delta^{15}\text{N}$  cross plots and these have been updated several times (Kendall et al., 2015,  
272 2008; Xue et al., 2009b). However, the identification of the origin of nitrogen concentrations in  
273 groundwater only by using nitrate isotope techniques is complicated due to the presence of mixed  
274 input from point and non-point sources and the occurrence of biogeochemical processes (e.g.,

275 nitrification, denitrification), in the unsaturated zone and the water body, that may alter the initial  
 276 isotopic values of the nitrate sources (Chen et al., 2010; Curt et al., 2004; Kendall, 1998).  
 277 Denitrification is a process that results in an increase of nitrate  $\delta^{15}\text{N}$  and  $\delta^{18}\text{O}$  as concentration  
 278 decreases (Mariotti et al., 1981). The observed linear relationship between the  $\delta^{15}\text{N}$  and  $\delta^{18}\text{O}$  values  
 279 of the sampling points, as depicted in Figure 3, implies that denitrification probably occurred for the  
 280 wells: 6 and 26 sampled in spring 2014; 2 and 114 sampled in fall 2014; and 6 sampled in spring  
 281 2015 (Table S1).  
 282 Pending further developments in the delineation of the sources, a useful approach to support the  
 283 interpretation of isotopic hydrochemistry can come from socio-hydrogeology (Re, 2015). The  
 284 administration of structured interviews to wells' owners during *in situ* measurements, can provide  
 285 useful insights on the manure and fertilizers use (Tringali et al., 2017), and successfully complement  
 286 isotopic data (Re et al., 2017).



287  
 288 Figure 3. Stable isotope composition of dissolved nitrates in groundwater from the Grombalia Basin, with ranges for groundwater as  
 289 per (Kendall et al., 2008).

290 However, an open question still remains related to the distinction between manure and sewage  
 291 derived nitrates, due to their overlapping  $\delta^{15}\text{N}_{\text{NO}_3}$  values ( $\sim 10\text{--}15\text{‰}$  (Kendall et al., 2008)). To this  
 292 end, selected samples with enriched  $\delta^{15}\text{N}_{\text{NO}_3}$  and mostly belonging to the G3 group, were also  
 293 analysed for  $\delta^{11}\text{B}$  (Table 1).

294 As in the case of  $\delta^{15}\text{N}_{\text{NO}_3}$  and  $\delta^{18}\text{O}_{\text{NO}_3}$ , the comparison of  $\delta^{11}\text{B}$  of samples with references data, and  
 295 more specifically with the compositional fields reported in the literature (Tirez et al., 2010; Widory  
 296 et al., 2005, 2004) (Figure 4), often provides important insights on contamination origin. In the case  
 297 of the samples collected in the Grombalia aquifer however, some data could bias the appropriate  
 298 source identification, if not correctly interpreted and/or supported by an adequate land use  
 299 analysis,. For example, one sample (26;  $\delta^{11}\text{B} = 25.45 \text{‰}$ ) falls in the compositional range of hog  
 300 manure, even if the well is located in a region where pig farming is not present (as this is not a  
 301 dominant activity in the country).

302

303 *Table 1. Summary of the main features of the wells whose samples collected in spring 2015 were analyzed for  $\delta^{11}\text{B}$ . Ranges are*  
 304 *calculated for Electrical Conductivity values (as a proxy for salinity) and nitrate concentrations, based on the following percentiles:*  
 305 *(+++):  $\geq 75$ ; (++):  $\geq 50$  and  $< 75$ ; (+)  $\geq 25$  and  $< 50$ ; (-)  $< 25$ . Variability refers to the occurrence of significant variations in  $\text{NO}_3$*   
 306 *concentrations in the different sampling campaigns.*

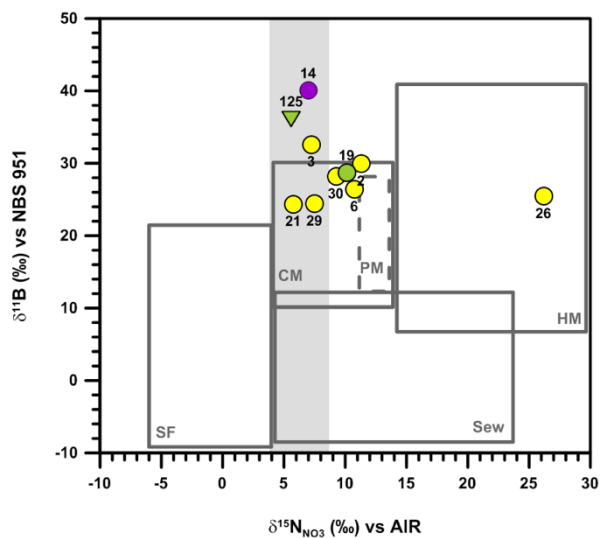
Well number	Area	Aquifer	Approx. distance from the sea (Km)	Salinity	Nitrates	Variability	$\delta^{11}\text{B}$ (‰)
2	Peri-urban	Shallow	3.0	++	++	NO	29.92
3	Peri-urban	Shallow	3.5	+++	++	YES	32.62
6	Rural	Shallow	9.3	+++	++	NO	26.41
14	Peri-urban	Shallow	11.8	+++	+++	NO	40.11
19	Rural	Shallow	13.7	+	++	NO	28.69
21	Rural	Shallow	17.9	++	++	YES	24.48
26	Rural	Shallow	18.5	++	+	NO	25.45
29	Rural	Shallow	12.7	++	++	NO	24.42
30	Peri-urban	Shallow	2.7	+++	+	NO	28.19
125	Rural	Deep	27.8	-	++	NO	36.10

307



308 Three samples (wells 3, 14, 125) plotting out of the literature manure compositional range, and  
 309 attributed to natural groundwater, show quite different hydrochemical characteristics, potentially  
 310 reflecting the interaction/mixing with different salinity sources (e.g. seawater and evaporites; Figure  
 311 4), and six samples (2, 6, 19, 21, 29, and 30) show an isotopic signature coherent with cattle manure.  
 312 However, as in the previous case, multiple sources are present (i.e. sewage, domestic effluents and  
 313 manure) that are not evidenced even by this coupled isotopic approach. Therefore, even though the  
 314 samples' selection for  $\delta^{11}\text{B}$  analyses was set with the overall goal of disaggregating the  
 315 contamination end-members in the mixing group (G3), the results did not permit to achieve it.  
 316 Additionally, this comparison reinforces what previously emerged from the  $\delta^{15}\text{N}_{\text{NO}_3}$  and  $\delta^{18}\text{O}_{\text{NO}_3}$   
 317 binary plot interpretation, and relates to the careful use of compositional ranges reported in the  
 318 literature. The latter indeed represent a valuable term of reference, but should not be considered  
 319 as the one and only landing point for data interpretation.

320



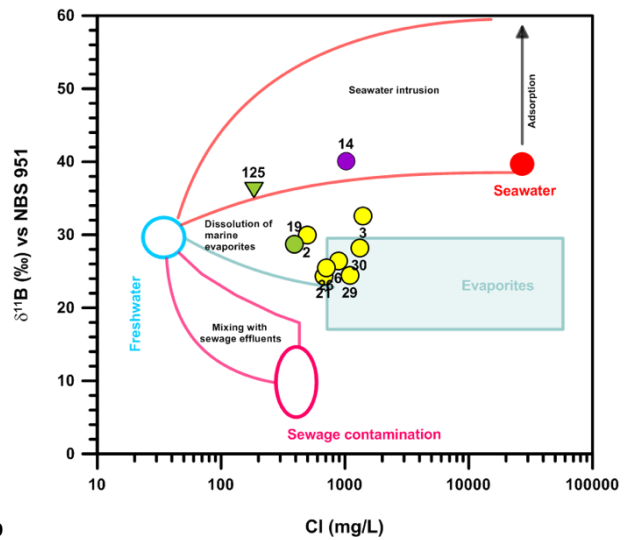
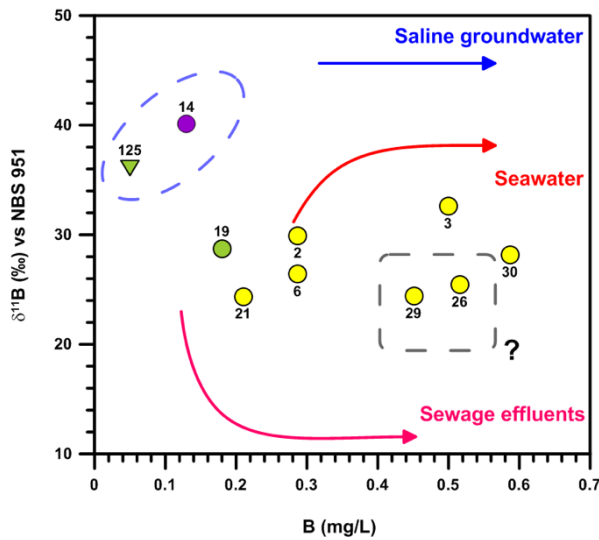
321

322 *Figure 4.  $\delta^{11}\text{B}$  vs  $\delta^{15}\text{N}$  of groundwater, for the samples collected in Fall 2015. Grey area = natural groundwater, SF: synthetic*  
 323 *fertilizers, Sew: sewage and septic plumes, CM: cattle manure, PM: poultry manure, HM: hog manure. (plot modified (Sacchi et al.,*  
 324 *2013)) compositional fields after (Widory et al., 2005, 2004), and (Tirez et al., 2010).*

325

326 To assist in the interpretation of  $\delta^{11}\text{B}$  values, plots versus the B or the Cl content have been used in  
327 the literature (Vengosh, 2014; Vengosh et al., 1994). In the case of our samples, the comparison  
328 between  $\delta^{11}\text{B}$  values and B concentrations permits to hypothesize the occurrence of seawater  
329 intrusion in the wells located near to the coast (2, 3 and 30; Figure 5a) and to highlight the impact  
330 of natural salinization in the recharge zone (well 125, and possibly to a lesser extent well 15, where  
331 the high salinity is also due to high nitrate concentrations). However, it is interesting to notice that,  
332 when comparing  $\delta^{11}\text{B}$  values with Cl concentrations (Figure 5b) different hypothesis can emerge on  
333 dominant processes. For example, the salinity of well number 3, where both the location near to  
334 the coast and the interview administration outcomes (Tringali et al., 2017) supports the  
335 aforementioned occurrence of saline water intrusion, could be attributed to the dissolution of  
336 marine evaporites. Similarly, wells 14 and 125, both quite far from the coast (Table 1), are probably  
337 affected by mixing with external saline sources (e.g. mixing with deeper brines/saline waters or  
338 evaporates), rather than mixing with (modern) seawater. For this reason, in A&SAR where  
339 evaporation processes and multiple sources of pollution can contribute to aquifer salinization, a  
340 careful approach to the use of  $\delta^{11}\text{B}$  literature data should be adopted when comparing results to  
341 reference values in order to avoid a biased attribution of dominant sources and processes, especially  
342 when B and Cl do not have a common origin.

343



344 Figure 5. (a)  $\delta^{11}\text{B}$  versus B concentrations compared to the processes evidenced by (Vengosh et al., 1994); (b)  $\delta^{11}\text{B}$  versus Cl  
 345 concentrations, modified after (Vengosh, 2014).

346

347 Results therefore show, as emerged in a similar geographical context (Re and Sacchi, 2017), that the  
 348 high geochemical background for B (min [B]= 0.053 mg/L, max = 1.041 mg/L; average = 0.319 mg/l,  
 349 Std Dev = 0.216) and Cl (min [Cl]= 57.6 mg/L, max = 2889.3 mg/L; average = 687.61 mg/l, Std Dev =  
 350 550.2), associated to complex water-rock interaction processes, limit the application of the coupled  
 351  $\delta^{11}\text{B}$  and  $\delta^{15}\text{N}$  isotopic systematics for the detection of groundwater nitrate pollution sources. In  
 352 fact, despite the exceedingly high nitrate contents of both agricultural and civil origin, the depleted  
 353  $\delta^{11}\text{B}$  values that characterize synthetic fertilizers (-10 to +20 ‰) and sewage leakages (-9 to +12  
 354 ‰) could not be detected. In this context, it may become fundamental not only looking at the  
 355 potential sources of contamination, but also at the ongoing processes. In fact, if, on one hand,  $\text{NO}_3$   
 356 input and nitrification can fuel up water-rock interaction processes and consequently favour  
 357 carbonate dissolution due to acidification of the solution, on the other hand, denitrification  
 358 produces alkalinity and fosters the re-precipitation of carbonates. While B incorporation into calcite  
 359 enriches the solid phase in  $^{11}\text{B}$  with respect to seawater, the dissolution of marine carbonates or of

360 secondary carbonates precipitated in the aquifers by freshwater would result in groundwater with  
361 lower  $\delta^{11}\text{B}$  values (Vengosh, 2010).  
362 Additionally, cation exchange and carbonate dissolution trigger B sorption on clays, thus  
363 contributing to the variation of the  $\delta^{11}\text{B}$  composition of groundwater. Indeed, exchange or sorption  
364 on clays favours  $^{10}\text{B}$  and is accompanied by an increase in  $^{11}\text{B}$  in the residual solution, potentially  
365 leading to considerable  $^{11}\text{B}$  enrichment coupled to a decrease in B content and in B/Cl ratios  
366 (Kloppmann et al., 2015). This could be the case, for example of samples 14 and 125 collected in the  
367 Grombalia aquifer. Another possible explanation, that may require further investigation, is the  
368 presence of deeper and older waters (with high  $\delta^{11}\text{B}$  and low B/Cl), originated from coastal air  
369 masses and undergone limited water-rock interaction with the matrix, that is mixing with the more  
370 recent waters located near to the recharge zone (e.g. well 125, approx. 28 Km from the coast).  
371 In summary, several processes affect the Boron content and isotope systematics, contributing to  
372 uncouple it from the nitrate isotope systematics and reducing its effectiveness for the identification  
373 of the sources of nitrate contamination.

374

#### 375 **Assessment of proportional source contribution using Bayesian isotope mixing modelling**

376 Two isotopes ( $j = 2$ ) ( $\delta^{15}\text{N}$  and  $\delta^{18}\text{O}$  of  $\text{NO}_3$ ) and three potential  $\text{NO}_3$  sources (nitrified synthetic  
377 fertilizers, synthetic fertilizers, and anthropogenic organic matter from manure and septic wastes)  
378 were considered in this study to estimate the contribution of  $\text{NO}_3$  sources in the sampling points of  
379 the two aquifers. The three potential  $\text{NO}_3$  source values were obtained from literature (Table 2).

380

381

382

383

384 *Table 2. End-members of  $\delta^{15}\text{N}$  and  $\delta^{18}\text{O}$  designated for the mixing models*

Source	$\delta^{15}\text{N}\text{-NO}_3$ (‰)	$\delta^{18}\text{O}\text{-NO}_3$ (‰)	References
Nitrified synthetic fertilizers	+0.4±2.0 (model 1)	+4.0±2.0	(Kendall et al., 2008)
	+4.5 ±1.0 (model 2)	+4.0±2.0	This study
Synthetic fertilizers	+0.4±2.0	+22.0±2.0	(Kendall et al., 2008)
Anthropogenic organic matter OM (manure-septic wastes)	+12.0±3.0	+7.0±2.0	(Kendall et al., 2008)

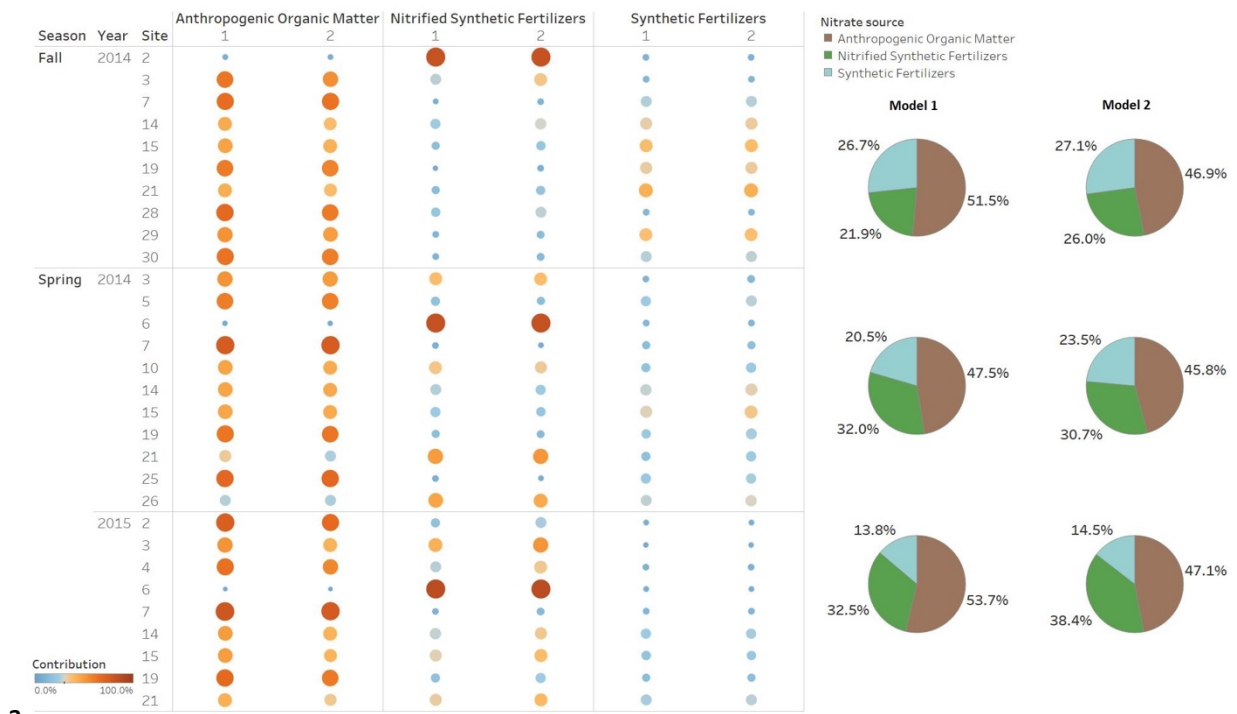
385

386 As previously mentioned, since denitrification is limited to a few samples only, corresponding  
 387 experiments for determining enrichment factors of denitrification were not conducted in this study.  
 388 Thus, a fractionation factor of 26 ‰ for  $\delta^{15}\text{N}$  and 12 ‰ for  $\delta^{18}\text{O}$  were assumed in Equation 1, based  
 389 on (Divers et al., 2014).

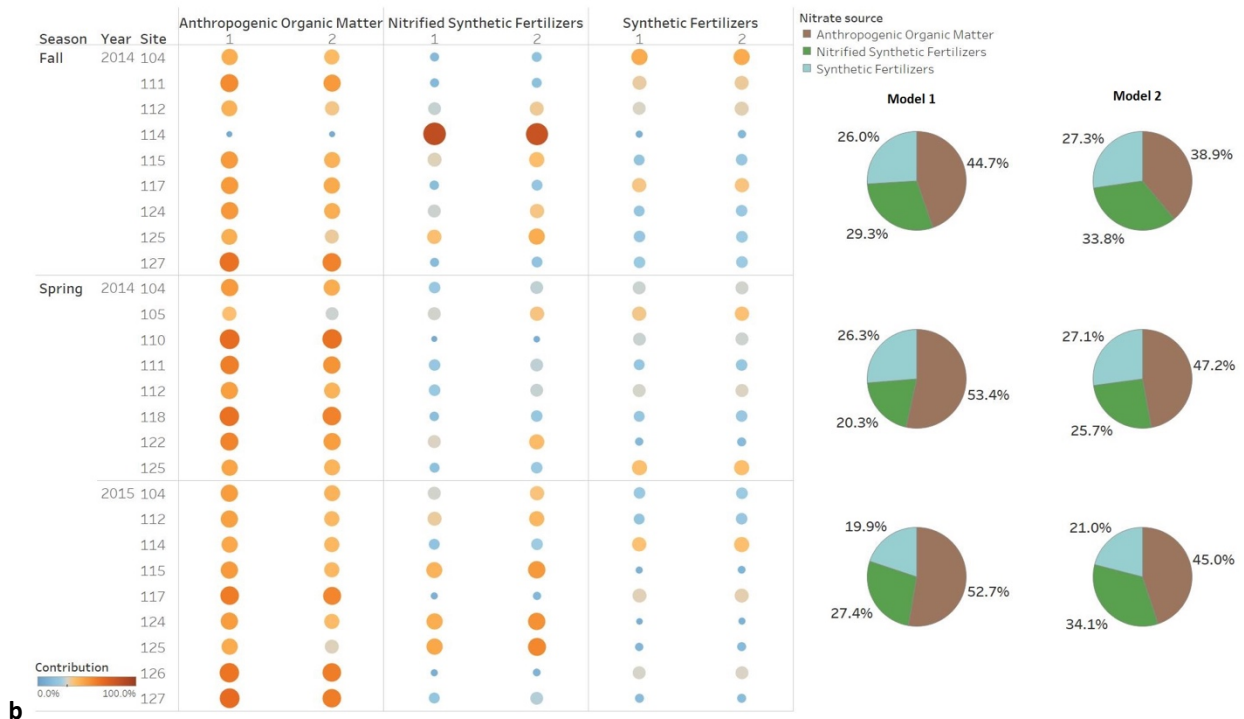
390 Additionally, two models were run with a different value attributed to  $\delta^{15}\text{N}$  of Nitrified Synthetic  
 391 Fertilizers (Table 2). Model 1 was run using an average value of +0.4±2.0 ‰ as per (Kendall et al.,  
 392 2008). In model 2 the end-member was chosen to be representative of the local conditions, thus a  
 393 value of +4.5±1.0 ‰ was selected based on the results of the current isotopic assessment (Figure 3,  
 394 Table S1). Indeed, in groundwater samples no  $\delta^{15}\text{N}$  values lower than +4 were found. Synthetic  
 395 fertilizers and anthropogenic organic matter were left unchanged in both models, as there are not  
 396 evidences for a change in A&SAR.

397 The Bayesian isotope mixing model suggested the predominant sources of nitrate in the two  
 398 aquifers (Figure 6). There was a relatively higher contribution from anthropogenic organic matter in  
 399 the shallow aquifer in 2014 and 2015, compared to other two sources. The proportional  
 400 contribution of the aforementioned source in both models 1 and 2 increased in spring 2015  
 401 compared to spring of 2014 (~2-6 %), which implies a continuous increase in the application of  
 402 manure or release of septic wastes in the region. Nitrified synthetic fertilizers and synthetic  
 403 fertilizers are less profound sources of nitrogen pollution in the shallow aquifer, and their  
 404 proportional contribution is not constant throughout the year, because it is related to the adopted

405 fertilization strategies. The models also showed that anthropogenic organic matter is the major  
406 source of nitrogen pollution for the deeper aquifer. The proportional contribution of organic matter  
407 in the deep aquifer showed seasonality, with the highest values observed in spring and the lowest  
408 ones in fall, which indicates that the impact of manure application or septic waste disposal is mostly  
409 observed when the deep aquifer is recharged. As for the shallow aquifer, the contribution of nitrified  
410 synthetic fertilizers and synthetic fertilizers is not as significant as the OM, and their proportional  
411 contribution depends on the fertilization strategies followed. The SIAR model gives an estimation of  
412 the proportional contribution, as it incorporates high uncertainty. The comparison of the two  
413 models highlights the need to determine the local nitrate isotope end-members given that  
414 estimates of the relative contributions of nitrate sources could be affected by any departures in  
415 isotopic composition of potential sources and the values we used (Figure 6). For example, the two  
416 models showed evident difference in the proportional contribution of the nitrate sources in the  
417 deep aquifer system. However, both models ranked anthropogenic organic matter as the  
418 predominant source of nitrogen pollution regardless the season and the year (Figure 6b). These  
419 differences, relevant both at whole aquifer and single well (e.g. anthropogenic organic matter  
420 ranked > 65% in samples 7 and 25 of the shallow aquifer, whereas nitrified synthetic fertilizers  
421 contributed > 80% in samples 6 and 114 of the shallow and the deep aquifer, respectively) level,  
422 may have important consequences if the mixing outcomes are used to support management  
423 strategies for nitrate contamination reduction. The effect of the uncorrected attribution of the  
424 dominant pollution sources may not only hamper the effective decrease in NO<sub>3</sub> levels in  
425 groundwater, but also create a sense of discontentment of local stakeholders and decrease in  
426 scientists and local institutions that are imposing constraints to local populations without meeting  
427 the promised goals.



a



b

428 Figure 6. Comparison of the proportional estimated contributions of N sources (synthetic fertilizers, nitrified synthetic fertilizers, and  
 429 anthropogenic organic matter) to nitrate in the shallow (a) and deep (b) aquifer sampled in 2014 and 2015. Model 1: using literature  
 430 data  $\delta^{15}N$  values from synthetic fertilizers; Model 2:  $\delta^{15}N$  value for synthetic fertilizers selected from the Grombalia aquifer data.

431

432

433 **Conclusion**

434 Results of the integrated approach applied to the Grombalia case study permits to highlight the  
 435 limitations of widely used techniques for nitrate source identification and apportionment in A&SAR  
 436 (Table 3), and allow the selection of the best combination of tools as a function of the project goals.  
 437 This would permit to maximize the benefits of the applications of these techniques, to identify the  
 438 most effective approach to be used for each case study, and ensure that hydrogeochemical  
 439 assessments would provide sound advices for improving the quality of local water resources and  
 440 prevent future contamination episodes.

441

442 *Table 3. Synthesis of the strengths and weaknesses of widely used techniques for nitrate source identification and apportionment in*  
 443 *arid and semi-arid regions.*

<b>Technique</b>	<b>Goal</b>	<b>Main strengths</b>	<b>Weakness</b>
<b>General chemistry</b>	To point out NO <sub>3</sub> contamination occurrence	Formulates a preliminary assumption of potential NO <sub>3</sub> origin	Does not allow to separate NO <sub>3</sub> and salinity
<b>Geochemical cartography and land use assessment</b>	To highlight the spatial distribution of NO <sub>3</sub> concentrations	Formulates a preliminary assumption of potential NO <sub>3</sub> origin	The outcome is highly dependent on the quality of the monitoring network (e.g. spatial distribution)  Do not allow to separate NO <sub>3</sub> and salinity
<b>Multivariate Statistical Analysis</b>	To unveil common patterns among samples	Groups samples based on their dominant characteristics (particularly useful with big data sets)	Does not offer easily accessible information about the chemical composition of the samples in the clusters (groups) (Güler et al., 2002);  Does not allow to separate NO <sub>3</sub> and salinity
<b>Dual nitrate isotopes (<math>\delta^{15}\text{N}_{\text{NO}_3}</math> and <math>\delta^{18}\text{O}_{\text{NO}_3}</math>)</b>	In depth identification of possible NO <sub>3</sub> sources	Unveils sources and occurrence of denitrification processes	Possible biased result interpretation due to poor literature on sources' characteristics, and post application modifications in A&SAR;  Do not allow to distinguish between sewage and manure
<b>Socio-hydrogeological approach</b>	In depth assessment of local application of fertilizers and manure	Cross checks with $\delta^{15}\text{N}$ and possible alternative when research funds are limited	Time consuming and requires specific training on public engagement theory
<b>Coupled <math>\delta^{15}\text{N}_{\text{NO}_3}</math> and <math>\delta^{11}\text{B}</math> systematics</b>	To discriminate among manure and sewage sources of NO <sub>3</sub>	Clear distinction of sewage and manure sources	Unsuitable for groundwater with high B geochemical background.
<b>Bayesian mixing modelling</b>	NO <sub>3</sub> source apportionment	Provides useful information on proportional contribution of each source, useful to support effective strategies for NO <sub>3</sub> contamination reduction	Highly dependent on the value attributed to the sources.



444

445 Overall, the use of integrated approaches is fundamental for supporting sustainable groundwater  
446 management, but, even in the case of well consolidated methodologies, results should be  
447 interpreted taking into account regional and local features.

448

#### 449 **Acknowledgments**

450 This research was supported by a Marie Curie International Outgoing Fellowship awarded to Dr.  
451 Viviana Re within the EU 7th FP for Research and Technological Development (FP7-PEOPLE-2012-  
452 IOF n. 327287). Isotopic Analysis ( $\delta^2\text{H}$ ,  $\delta^{18}\text{O}$ ) were carried within the framework of the Technical  
453 cooperation project with the International Atomic Energy Agency, TUN 7003: “Using Isotope Tracers  
454 Techniques for Integrated Sustainable Groundwater Management (2016-2018)”.

455

#### 456 **References.**

457 Alsharhan, A.S., Rizk, Z.E., 2020. Water Resources and Integrated Management of the United Arab  
458 Emirates, World Water Resources. Springer International Publishing, Cham.

459 <https://doi.org/10.1007/978-3-030-31684-6>

460 Ben Moussa, A., Salem, S.B.H., Zouari, K., Jlassi, F., 2010. Hydrochemical and isotopic investigation  
461 of the groundwater composition of an alluvial aquifer, Cap Bon Peninsula, Tunisia.

462 Carbonates and Evaporites 25, 161–176. <https://doi.org/10.1007/s13146-010-0020-7>

463 Ben Moussa, A., Zouari, K., 2011. Hydrochemical Investigation of Groundwater Contamination in  
464 the Grombalia Shallow Aquifer, Cap Bon Peninsula, Tunisia: Impact of Irrigation with  
465 Industrial Waste Water, in: Waste Water - Evaluation and Management. InTech.

466 <https://doi.org/10.5772/15837>

467 Castany, G., 1948. Les fosses d’effondrement de Tunisie géologie et hydrologie. Impr. S.A.P.I,

468 Tunis.

469 Charfi, S., Trabelsi, R., Zouari, K., Chkir, N., Charfi, H., Rekaia, M., 2013. Isotopic and hydrochemical  
470 investigation of the Grombalia deep aquifer system, northeastern Tunisia. Carbonates and  
471 Evaporites. <https://doi.org/10.1007/s13146-012-0114-5>

472 Chatfield, C., 2018. Introduction to multivariate analysis.

473 Chen, Weiqi, Chen, Weicai, Rao, H., Zhang, L., Hong, H., 2010. An improved ion-exchange/diffusion  
474 method for  $^{15}\text{N}$  isotope tracing analysis of nitrate in surface waters from watersheds. J.  
475 Environ. Sci. 22, 784–788. [https://doi.org/10.1016/S1001-0742\(09\)60177-7](https://doi.org/10.1016/S1001-0742(09)60177-7)

476 Chenini, I., Zghibi, A., Kouzana, L., 2015. Hydrogeological investigations and groundwater  
477 vulnerability assessment and mapping for groundwater resource protection and  
478 management: State of the art and a case study. J. African Earth Sci. 109, 11–26.  
479 <https://doi.org/10.1016/j.jafrearsci.2015.05.008>

480 Craine, J.M., Brookshire, E.N.J., Cramer, M.D., Hasselquist, N.J., Koba, K., Marin-Spiotta, E., Wang,  
481 L., 2015. Ecological interpretations of nitrogen isotope ratios of terrestrial plants and soils.  
482 Plant Soil. <https://doi.org/10.1007/s11104-015-2542-1>

483 Curt, M.D., Aguado, P., Sánchez, G., Bigeriego, M., Fernández, J., 2004. Nitrogen isotope ratios of  
484 synthetic and organic sources of nitrate water contamination in Spain. Water. Air. Soil Pollut.  
485 151, 135–142. <https://doi.org/10.1023/B:WATE.0000009889.36833.c0>

486 Danni, S.O., Bouchaou, L., Elmouden, A., Brahim, Y.A., N'da, B., 2019. Assessment of water quality  
487 and nitrate source in the Massa catchment (Morocco) using  $\delta^{15}\text{N}$  and  $\delta^{18}\text{O}$  tracers. Appl.  
488 Radiat. Isot. 154, 108859. <https://doi.org/10.1016/j.apradiso.2019.108859>

489 Deutsch, B., Mewes, M., Liskow, I., Voss, M., 2006. Quantification of diffuse nitrate inputs into a  
490 small river system using stable isotopes of oxygen and nitrogen in nitrate. Org. Geochem. 37,  
491 1333–1342. <https://doi.org/10.1016/j.orggeochem.2006.04.012>

492 Diédhiou, M., Cissé Faye, S., Diouf, O.C., Faye, S., Faye, A., Re, V., Wohnlich, S., Wisotzky, F.,  
493 Schulte, U., Maloszewski, P., 2012. Tracing groundwater nitrate sources in the Dakar  
494 suburban area: An isotopic multi-tracer approach. *Hydrol. Process.* 26, 760–770.  
495 <https://doi.org/10.1002/hyp.8172>

496 Divers, M.T., Elliott, E.M., Bain, D.J., 2014. Quantification of nitrate sources to an urban stream  
497 using dual nitrate isotopes. *Environ. Sci. Technol.* 48, 10580–10587.  
498 <https://doi.org/10.1021/es404880j>

499 Edmunds, W.M., Shand, P., 2009. *Natural Groundwater Quality, Natural Groundwater Quality.*  
500 wiley, Oxford, UK. <https://doi.org/10.1002/9781444300345>

501 Favreau, G., Cappelaere, B., Massuel, S., Leblanc, M., Boucher, M., Boulain, N., Leduc, C., 2009.  
502 Land clearing, climate variability, and water resources increase in semiarid southwest Niger: A  
503 review. *Water Resour. Res.* 45. <https://doi.org/10.1029/2007WR006785>

504 Gaaloul, N., Candela, L., Chebil, A., Soussi, A., Tamoh, K., 2014. Groundwater flow simulation at the  
505 Grombalia phreatic aquifer (Cap Bon, Northeastern Tunisia). *Desalin. Water Treat.* 52, 1997–  
506 2008. <https://doi.org/10.1080/19443994.2013.821026>

507 Gonfiantini, R., Stichler, W., Rozanski, K., 1995. Standards and intercomparison materials  
508 distributed by the. *Isot. Hydrol. Sec.*

509 Greene, R., Timms, W., Rengasamy, P., Arshad, M., Cresswell, R., 2016. Soil and aquifer  
510 salinization: Toward an integrated approach for salinity management of groundwater, in:  
511 *Integrated Groundwater Management: Concepts, Approaches and Challenges.* Springer  
512 International Publishing, pp. 377–412. [https://doi.org/10.1007/978-3-319-23576-9\\_15](https://doi.org/10.1007/978-3-319-23576-9_15)

513 Güler, C., Thyne, G.D., McCray, J.E., Turner, A.K., 2002. Evaluation of graphical and multivariate  
514 statistical methods for classification of water chemistry data. *Hydrogeol. J.* 10, 455–474.  
515 <https://doi.org/10.1007/s10040-002-0196-6>

516 Gutiérrez, M., Biagioni, R.N., Alarcón-Herrera, M.T., Rivas-Lucero, B.A., 2018. An overview of  
517 nitrate sources and operating processes in arid and semiarid aquifer systems. *Sci. Total*  
518 *Environ.* <https://doi.org/10.1016/j.scitotenv.2017.12.252>

519 IPCC, 2021. AR6 Climate Change 2021: Impacts, Adaptation and Vulnerability [WWW Document].  
520 Intergov. Panel Clim. Chang. Contrib. Work. Gr. II to Third Assess. Rep. Intergov. Panel Clim.  
521 Chang. URL <https://www.ipcc.ch/report/sixth-assessment-report-working-group-ii/>

522 Isonitrate, 2010. ISONITRATE- - Improved management of nitrate pollution in water using isotopic  
523 monitoring LIFE06 ENV/F/000158 [WWW Document]. *Appl. Note.* URL  
524 [https://ec.europa.eu/environment/life/project/Projects/index.cfm?fuseaction=search.dspPa](https://ec.europa.eu/environment/life/project/Projects/index.cfm?fuseaction=search.dspPage&n_proj_id=3107)  
525 [ge&n\\_proj\\_id=3107](https://ec.europa.eu/environment/life/project/Projects/index.cfm?fuseaction=search.dspPage&n_proj_id=3107) (accessed 7.16.20).

526 Jackson, A.L., Inger, R., Bearhop, S., Parnell, A., 2009. Erroneous behaviour of MixSIR, a recently  
527 published Bayesian isotope mixing model: A discussion of Moore & Semmens (2008). *Ecol.*  
528 *Lett.* 12, E1–E5. <https://doi.org/10.1111/j.1461-0248.2008.01233.x>

529 Jalali, M., 2007. Salinization of groundwater in arid and semi-arid zones: An example from Tajarak,  
530 western Iran. *Environ. Geol.* 52, 1133–1149. <https://doi.org/10.1007/s00254-006-0551-3>

531 Kaiser, H.F., 1958. The varimax criterion for analytic rotation in factor analysis. *Psychometrika* 23,  
532 187–200. <https://doi.org/10.1007/BF02289233>

533 Kammoun, S., Re, V., Trabelsi, R., Zouari, K., Daniele, S., 2018a. Assessing seasonal variations and  
534 aquifer vulnerability in coastal aquifers of semi-arid regions using a multi-tracer isotopic  
535 approach: the case of Grombalia (Tunisia). *Hydrogeol. J.* 26, 2575–2594.  
536 <https://doi.org/10.1007/s10040-018-1816-0>

537 Kammoun, S., Trabelsi, R., Re, V., Zouari, K., Henchiri, J., 2018b. Groundwater quality assessment  
538 in semi-arid regions using integrated approaches: the case of Grombalia aquifer (NE Tunisia).  
539 *Environ. Monit. Assess.* <https://doi.org/10.1007/s10661-018-6469-x>

540 Kendall, C., 1998. Tracing Nitrogen Sources and Cycling in Catchments, in: Isotope Tracers in  
541 Catchment Hydrology. Elsevier, pp. 519–576. [https://doi.org/10.1016/b978-0-444-81546-](https://doi.org/10.1016/b978-0-444-81546-0.50023-9)  
542 [0.50023-9](https://doi.org/10.1016/b978-0-444-81546-0.50023-9)

543 Kendall, C., Aravena, R., 2000. Nitrate Isotopes in Groundwater Systems, in: Environmental Tracers  
544 in Subsurface Hydrology. Springer US, pp. 261–297. [https://doi.org/10.1007/978-1-4615-](https://doi.org/10.1007/978-1-4615-4557-6_9)  
545 [4557-6\\_9](https://doi.org/10.1007/978-1-4615-4557-6_9)

546 Kendall, C., Elliott, E.M., Wankel, S.D., 2008. Tracing Anthropogenic Inputs of Nitrogen to  
547 Ecosystems, in: Stable Isotopes in Ecology and Environmental Science: Second Edition.  
548 Blackwell Publishing Ltd, pp. 375–449. <https://doi.org/10.1002/9780470691854.ch12>

549 Kendall, C., Young, M.B., Silva, S.R., Kraus, T.E.C., Peek, S., Guerin, M., 2015. Tracing nutrient and  
550 organic matter sources and biogeochemical processes in the Sacramento River and Northern  
551 Delta: proof of concept using stable isotope data. U.S. Geol. Surv. 1–106.  
552 <https://doi.org/http://dx.doi.org/10.5066/F7QJ7FCM>

553 Kloppmann, W., Petelet-Giraud, E., Guerrot, C., Cary, L., Pauwels, H., 2015. Extreme Boron Isotope  
554 Ratios in Groundwater. Procedia Earth Planet. Sci. 13, 296–300.  
555 <https://doi.org/10.1016/j.proeps.2015.07.069>

556 Leduc, C., Pulido Bosch, A., Remini, B., Massuel, S., 2018. Sub-chapter 2.3.5. Changes in  
557 Mediterranean groundwater resources, in: The Mediterranean Region under Climate Change.  
558 IRD Éditions, pp. 327–333. <https://doi.org/10.4000/books.irdeditions.23583>

559 Mariotti, A., Germon, J.C., Hubert, P., Kaiser, P., Letolle, R., Tardieux, A., Tardieux, P., 1981.  
560 Experimental determination of nitrogen kinetic isotope fractionation: Some principles;  
561 illustration for the denitrification and nitrification processes. Plant Soil 62, 413–430.  
562 <https://doi.org/10.1007/BF02374138>

563 Martinelli, G., Dadomo, A., De Luca, D.A., Mazzola, M., Lasagna, M., Pennisi, M., Pilla, G., Sacchi, E.,

564 Saccon, P., 2018. Nitrate sources, accumulation and reduction in groundwater from Northern  
565 Italy: Insights provided by a nitrate and boron isotopic database. *Appl. Geochemistry* 91, 23–  
566 35. <https://doi.org/10.1016/j.apgeochem.2018.01.011>

567 Matiatos, I., 2016. Nitrate source identification in groundwater of multiple land-use areas by  
568 combining isotopes and multivariate statistical analysis: A case study of Asopos basin (Central  
569 Greece). *Sci. Total Environ.* 541, 802–814. <https://doi.org/10.1016/j.scitotenv.2015.09.134>

570 Meghdadi, A., Javar, N., 2018. Quantification of spatial and seasonal variations in the proportional  
571 contribution of nitrate sources using a multi-isotope approach and Bayesian isotope mixing  
572 model. *Environ. Pollut.* 235, 207–222. <https://doi.org/10.1016/j.envpol.2017.12.078>

573 Moore, J.W., Semmens, B.X., 2008. Incorporating uncertainty and prior information into stable  
574 isotope mixing models. *Ecol. Lett.* 11, 470–480. [https://doi.org/10.1111/j.1461-  
575 0248.2008.01163.x](https://doi.org/10.1111/j.1461-0248.2008.01163.x)

576 Mortimore, M., With, C., Anderson, S., Cotula, L., Davies, J., Faccar, K., Hesse, C., Morton, J.,  
577 Nyangena, W., Skinner, J., Wolfangel, C., 2009. Dryland Opportunities: A new paradigm for  
578 people, ecosystems and development.

579 Parnell, A.C., Inger, R., Bearhop, S., Jackson, A.L., 2010. Source partitioning using stable isotopes:  
580 Coping with too much variation. *PLoS One*. <https://doi.org/10.1371/journal.pone.0009672>

581 Penna, D., Stenni, B., Šanda, M., Wrede, S., Bogaard, T.A., Gobbi, A., Borga, M., Fischer, B.M.C.,  
582 Bonazza, M., Chárová, Z., 2010. On the reproducibility and repeatability of laser absorption  
583 spectroscopy measurements for  $\delta^2\text{H}$  and  $\delta^{18}\text{O}$  isotopic analysis. *Hydrol. Earth Syst. Sci.* 14,  
584 1551–1566. <https://doi.org/10.5194/hess-14-1551-2010>

585 Phillips, D.L., Gregg, J.W., 2003. Source partitioning using stable isotopes: Coping with too many  
586 sources. *Oecologia* 136, 261–269. <https://doi.org/10.1007/s00442-003-1218-3>

587 Phillips, D.L., Koch, P.L., 2002. Incorporating concentration dependence in stable isotope mixing

588 models. *Oecologia* 130, 114–125. <https://doi.org/10.1007/s004420100786>

589 Re, V., 2015. Incorporating the social dimension into hydrogeochemical investigations for rural  
590 development: the Bir Al-Nas approach for socio-hydrogeology. *Inc. la Dimens. Soc. en las*  
591 *Investig. hidrogeológicas para el Desarro. Rural el enfoque Bir Al-Nas para la socio-*  
592 *hidrogeología.*

593 Re, V., Sacchi, E., 2017. Tackling the salinity-pollution nexus in coastal aquifers from arid regions  
594 using nitrate and boron isotopes. *Environ. Sci. Pollut. Res.* [https://doi.org/10.1007/s11356-](https://doi.org/10.1007/s11356-017-8384-z)  
595 [017-8384-z](https://doi.org/10.1007/s11356-017-8384-z)

596 Re, V., Sacchi, E., Kammoun, S., Tringali, C., Trabelsi, R., Zouari, K., Daniele, S., 2017. Integrated  
597 socio-hydrogeological approach to tackle nitrate contamination in groundwater resources.  
598 The case of Grombalia Basin (Tunisia). *Sci. Total Environ.* 593–594, 664–676.  
599 <https://doi.org/10.1016/j.scitotenv.2017.03.151>

600 Re, V., Zuppi, G.M., 2011. Influence of precipitation and deep saline groundwater on the  
601 hydrological systems of Mediterranean coastal plains: a general overview. *Hydrol. Sci. J.* 56,  
602 966–980. <https://doi.org/10.1080/02626667.2011.597355>

603 Sacchi, E., Acutis, M., Bartoli, M., Brenna, S., Delconte, C.A., Laini, A., Pennisi, M., 2013. Origin and  
604 fate of nitrates in groundwater from the central Po plain: Insights from isotopic  
605 investigations. *Appl. Geochemistry* 34, 164–180.  
606 <https://doi.org/10.1016/j.apgeochem.2013.03.008>

607 Silva, S.R., Kendall, C., Wilkison, D.H., Ziegler, A.C., Chang, C.C.Y., Avanzino, R.J., 2000. A new  
608 method for collection of nitrate from fresh water and the analysis of nitrogen and oxygen  
609 isotope ratios. *J. Hydrol.* 228, 22–36. [https://doi.org/10.1016/S0022-1694\(99\)00205-X](https://doi.org/10.1016/S0022-1694(99)00205-X)

610 Slama, T., Sebei, A., 2020. Spatial and temporal analysis of shallow groundwater quality using GIS,  
611 Grombalia aquifer, Northern Tunisia. *J. African Earth Sci.* 170, 103915.

612 <https://doi.org/10.1016/j.jafrearsci.2020.103915>

613 Spalding, R.F., Exner, M.E., 1993. Occurrence of Nitrate in Groundwater—A Review. *J. Environ.*  
614 *Qual.* 22, 392–402. <https://doi.org/10.2134/jeq1993.00472425002200030002x>

615 Stock, B.C., Jackson, A.L., Ward, E.J., Parnell, A.C., Phillips, D.L., Semmens, B.X., 2018. Analyzing  
616 mixing systems using a new generation of Bayesian tracer mixing models.  
617 <https://doi.org/10.7287/peerj.preprints.26884v1>

618 Tirez, K., Brusten, W., Widory, D., Petelet, E., Bregnot, A., Xue, D., Boeckx, P., Bronders, J., 2010.  
619 Boron isotope ratio ( $\delta^{11}\text{B}$ ) measurements in Water Framework Directive monitoring  
620 programs: Comparison between double focusing sector field ICP and thermal ionization mass  
621 spectrometry. *J. Anal. At. Spectrom.* 25, 964–974. <https://doi.org/10.1039/c001840f>

622 Tringali, C., Re, V., Siciliano, G., Chkir, N., Tuci, C., Zouari, K., 2017. Insights and participatory  
623 actions driven by a socio-hydrogeological approach for groundwater management: the  
624 Grombalia Basin case study (Tunisia) Aperçus et actions participatives guidées par une  
625 approche socio-hydrogéologique pour la gestion des ressourc. *Hydrogeol. J.* 25, 1241–1255.  
626 <https://doi.org/10.1007/s10040-017-1542-z>

627 Vengosh, A., 2014. 1.9 Salinization and Saline Environments. *Treatise on Geochemistry* 325–378.  
628 <https://doi.org/10.1016/B978-0-08-095975-7.00909-8>

629 Vengosh, A., 2010. Boron isotopes as a proxy for carbonate dissolution in groundwater—  
630 radiocarbon correction models, in: *Water-Rock Interaction*. CRC Press, pp. 107–110.

631 Vengosh, A., Heumann, K.G., Juraske, S., Kasher, R., 1994. Boron Isotope Application for Tracing  
632 Sources of Contamination in Groundwater. *Environ. Sci. Technol.* 28, 1968–1974.  
633 <https://doi.org/10.1021/es00060a030>

634 Voss, M., Deutsch, B., Elmgren, R., Humborg, C., Kuuppo, P., Pastuszak, M., Rolff, C., Schulte, U.,  
635 2006. Source identification of nitrate by means of isotopic tracers in the Baltic Sea



636 catchments. *Biogeosciences* 3, 663–676. <https://doi.org/10.5194/bg-3-663-2006>

637 WHO, 2011. Guidelines for Drinking-water Quality FOURTH EDITION WHO Library Cataloguing-in-  
638 Publication Data Guidelines for drinking-water quality-4 th ed.

639 Widory, D., Kloppmann, W., Chery, L., Bonnin, J., Rochdi, H., Guinamant, J.L., 2004. Nitrate in  
640 groundwater: An isotopic multi-tracer approach. *J. Contam. Hydrol.* 72, 165–188.  
641 <https://doi.org/10.1016/j.jconhyd.2003.10.010>

642 Widory, D., Petelet-Giraud, E., Négrel, P., Ladouche, B., 2005. Tracking the sources of nitrate in  
643 groundwater using coupled nitrogen and boron isotopes: A synthesis. *Environ. Sci. Technol.*  
644 39, 539–548. <https://doi.org/10.1021/es0493897>

645 Xia, Y., Li, Y., Zhang, X., Yan, X., 2017. Nitrate source apportionment using a combined dual  
646 isotope, chemical and bacterial property, and Bayesian model approach in river systems. *J.*  
647 *Geophys. Res. Biogeosciences* 122, 2–14. <https://doi.org/10.1002/2016JG003447>

648 Xue, D., Botte, J., De Baets, B., Accoe, F., Nestler, A., Taylor, P., Van Cleemput, O., Berglund, M.,  
649 Boeckx, P., 2009a. Present limitations and future prospects of stable isotope methods for  
650 nitrate source identification in surface- and groundwater. *Water Res.*  
651 <https://doi.org/10.1016/j.watres.2008.12.048>

652 Xue, D., Botte, J., De Baets, B., Accoe, F., Nestler, A., Taylor, P., Van Cleemput, O., Berglund, M.,  
653 Boeckx, P., 2009b. Present limitations and future prospects of stable isotope methods for  
654 nitrate source identification in surface- and groundwater. *Water Res.*  
655 <https://doi.org/10.1016/j.watres.2008.12.048>

656 Yang, L., Han, J., Xue, J., Zeng, L., Shi, J., Wu, L., Jiang, Y., 2013. Nitrate source apportionment in a  
657 subtropical watershed using Bayesian model. *Sci. Total Environ.* 463–464, 340–347.  
658 <https://doi.org/10.1016/j.scitotenv.2013.06.021>

659 Zhang, Y., Shi, P., Li, F., Wei, A., Song, J., Ma, J., 2018. Quantification of nitrate sources and fates in

660 rivers in an irrigated agricultural area using environmental isotopes and a Bayesian isotope  
661 mixing model. *Chemosphere* 208, 493–501.  
662 <https://doi.org/10.1016/j.chemosphere.2018.05.164>  
663